

USE OF ADJACENT JETS TO INVESTIGATE THE AERODYNAMIC SOUND OF AIRFOILS AT MODERATELY HIGH REYNOLDS NUMBERS

H. ARBEY, M. SUNYACH AND G. COMTE-BELLOT

*Laboratoire de Mécanique des Fluides,
An Associated Laboratory of the Centre National de la Recherche Scientifique,
Ecole Centrale de Lyon, 69130 Ecully, France*

(Received 4 December 1978, and in revised form 27 February 1979)

A new experimental set-up is proposed to investigate the noise generated by airfoils. It consists of two adjacent plane jets ducted into an anechoic room, and the airfoils under investigation are placed in the median jet. Besides the benefit in the acoustical conditions of the experiments (decrease of the background noise due to the jets, shift of the preferred frequencies of the jets below the range of interest for the airfoil emission), the aerodynamic situation itself is improved (increase in length of the potential zone, decrease of induced flow fluctuations). There is therefore the possibility to investigate airfoil noise with longer chords and higher incident velocities.

1. INTRODUCTION

When investigating the aerodynamic sound generated by airfoils, one usually locates the airfoil either in a free jet ducted into an anechoic room [1–3] or in the test section of a wind tunnel [4–5]. In the latter case only near field acoustic measurements are possible. They are limited by the background noise of the installation and perturbed both by the flow and the reverberation due to the tunnel walls. These deficiencies will exist until we have techniques able to educe acoustic signals in confined spaces and in the presence of flows. In the free jet case, far field acoustic measurements are conveniently obtained along with the necessary aerodynamic characteristics. However, the jet noise limits the acoustic measurements because the jet section has to be large in comparison with the airfoil blocking area. Furthermore, an extension to high velocities is made difficult because the jet noise increases with speed at a faster rate than airfoil noise.

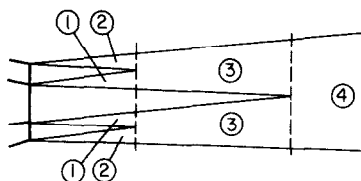
The authors therefore propose a new experimental set-up in which adjacent plane jets ducted into an anechoic room are used. This has been suggested by results from their previous work dealing with aerodynamic and acoustic properties of coaxial jets [6]. Because of the decrease of both the mean velocity gradient and the turbulent kinetic energy in the mixing zone between the primary and secondary flows, several advantages can be expected: (i) an overall noise level reduction for the jets; (ii) a shift towards lower frequencies of the jet noise spectra, i.e., away from the frequency range corresponding to the airfoil noise under investigation; (iii) an increase of the length of the potential zone of the primary jet; (iv) a decrease of the irrotational velocity fluctuations induced in that potential zone by the random motion of the primary jet boundaries.

Thus, if the airfoil is located in the median jet of an adjacent plane jets system, then, as compared to the case of a single jet with the same characteristics as the median jet alone, the airfoil chord can be chosen longer and the incident velocities higher, so that a high Reynolds number would be conveniently achieved. Feasibility experiments have been made on a small set-up. The results are presented in what follows (sections 4.1 to 4.3) and possible extensions to the present work discussed. The effects of the jet mixing layers on the transmission of the acoustic waves emitted by the airfoil have also been considered (section 4.4).

2. CHOICE OF THE JET SYSTEM

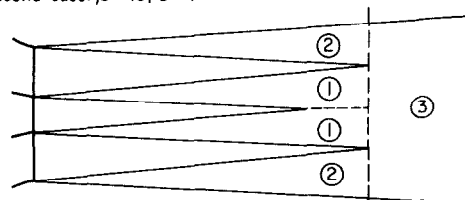
The characteristics of the system of adjacent jets have been chosen according to our recent analysis [6] which gives a semi-empirical law for the noise level reduction afforded by coaxial jets. For purposes of analysis, the flow is regarded as partitioned into several regions with specific relevant length and velocity scales (see Figure 1). Insofar as only aerodynamic aspects are concerned, the acoustic efficiency of the coaxial system has been defined by comparing the noise intensity I of the coaxial system to I_{th} , that of a single jet

First case: $\beta \leq 10, \delta < 1$



Zone number	Velocity scale	Length scale	Zone length
1	$U_p - U_s$	D_p	$5\gamma\delta D_p$
2	U_s	D_s	$5\gamma\delta D_p$
3	V	L	$5\gamma(1-\delta)D_p$
4	V	L	$5\gamma D_p$

Second case: $\beta > 10, \delta > 1$



Zone number	Velocity scale	Length scale	Zone length
1	$U_p - U_s$	D_p	$5\gamma\delta D_p$
2	U_s	D_s	$5\gamma\delta D_p$
3	V	L	$5\gamma\delta D_p$

Figure 1. Relevant parameters used in reference [6] for estimates of the noise emitted by coaxial jets.

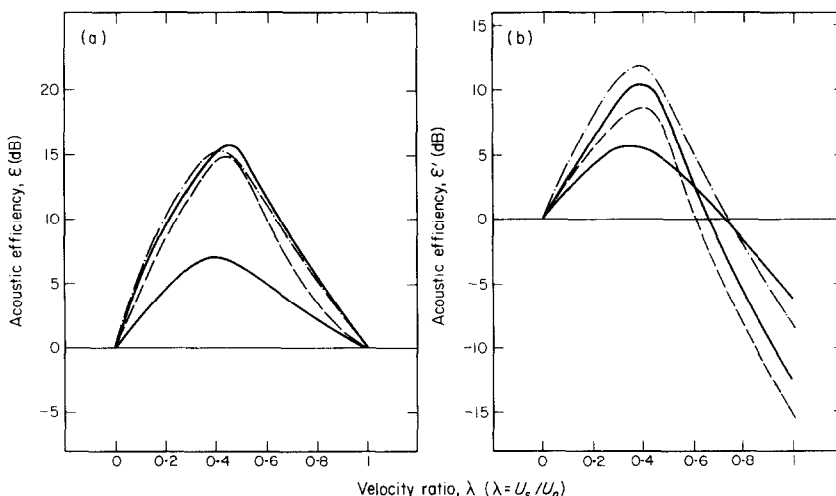


Figure 2. Acoustic efficiency of coaxial jets for different velocity ratio and different nozzle area ratio. (a) Acoustic efficiency $\varepsilon(\beta, \lambda)$ defined by expression (1); (b) acoustic efficiency $\varepsilon'(\beta, \lambda)$ defined by expression (3). —, $\beta = 2$; - - -, $\beta = 8$; ---, $\beta = 15$; ···, $\beta = 20$.

which would have the same velocity as the central jet together with the same thrust: i.e.,

$$\varepsilon = -10 \log(I/I_{th}) \tag{1}$$

(here I_{th} replaces I_r in reference [6]; we prefer the notation I_{th} because of the thrust condition and the different reference jet that we use). It has been shown [6] that ε can be expressed by

$$\varepsilon(\beta, \lambda) = -10 \log \left[\gamma \frac{\delta [(1-\lambda)^m + \lambda^m \sqrt{1+\beta}] + (2-\delta)(1+\beta\lambda^2)^{m-1/2} (1+\beta\lambda)^{1-m}}{2(1+\beta\lambda^2)} \right] \tag{2}$$

for $\beta \lesssim 10$, $\delta \lesssim 1$, and by

$$\varepsilon(\beta, \lambda) = -10 \log \left[\gamma \delta \left(\frac{(1-\lambda)^m + \lambda^m \sqrt{1+\beta} + (1+\beta\lambda^2)^{m-1/2} (1+\beta\lambda)^{1-m}}{2(1+\beta\lambda^2)} \right) \right] \tag{2'}$$

for $\beta > 10$, $\delta > 1$, where m is the power law exponent which expresses the noise dependence on velocity, λ is the ratio of the secondary to the primary velocity, β is the ratio of the secondary to the primary nozzle area, γ is the ratio between the lengths of the primary potential zone with and without the secondary jet (mainly a function of λ), and δ is the ratio between the length of the secondary potential zone and the length of the primary potential zone (a function of λ and β).

In this investigation the acoustic efficiency of the coaxial system can be more relevantly defined in respect to the noise intensity I_{pr} of the primary jet itself: i.e.,

$$\varepsilon' = -10 \log(I/I_{pr}). \tag{3}$$

Since I_{th} and I_{pr} are simply related through the ratio of the squared diameters of the constant thrust jet and the primary jet, which amounts to $1 + \beta\lambda^2$, ε' is related to ε by

$$\varepsilon' = \varepsilon - 10 \log(1 + \beta\lambda^2). \tag{4}$$

Plots of ε and ε' are given in Figure 2; positive values correspond to a noise reduction. It can be noted that ε' reaches a maximum for $\lambda \simeq 0.4$ and $\beta \simeq 10$, which, in the case of coaxial jets, allows a nearly equivalent and independent downstream evolution of the

primary and secondary potential zones. Larger values of β apparently leave the primary jet development unchanged but increase the overall noise emitted. Smaller values of β do not allow the secondary flow to act significantly on the primary jet whose noise is therefore not reduced as much as would be possible. When $\beta \simeq 10$ the diameter of the secondary jet is simply about three times the diameter of the primary jet and an extension to adjacent plane jets leads to a secondary nozzle which has the same width as the median jet: i.e., an area ratio $\beta' \simeq 2$. In addition, from a practical point of view, this low value of β' leads to mass and momentum rates for the secondary flow which are conveniently produced.

An extension of the semi-empirical analysis model to the adjacent plane jets system is possible by using the same partition of the flow and the same relevant length and velocity scales as for the coaxial jet system (see Figure 1), so that $\varepsilon(\beta', \lambda)$ can be expressed by

$$\varepsilon(\beta', \lambda) = -10 \log \left[\gamma \frac{\delta[(1-\lambda)^m + \lambda^m(1+\beta')] + (1+\beta'\lambda)^{2-m}(1+\beta'\lambda^2)^{m-1}(2-\delta)}{2(1+\beta'\lambda^2)^2} \right] \quad (5)$$

for $\beta' \leq 2$, $\delta \leq 1$, and by

$$\varepsilon(\beta', \lambda) = -10 \log \left[\gamma \delta \left(\frac{(1-\lambda)^m + \lambda^m(1+\beta') + (1+\beta'\lambda)^{2-m}(1+\beta'\lambda^2)^{m-1}}{2(1+\beta'\lambda^2)^2} \right) \right] \quad (5')$$

for $\beta' > 2$, $\delta < 1$. For ε' , one has, instead of equation (4),

$$\varepsilon' = \varepsilon - 10 \log(1 + \beta'\lambda^2)^2. \quad (6)$$

3. EXPERIMENTAL FACILITIES

The dimensions of the set-up have so far been kept small since only feasibility experiments were carried out. A 5 cm \times 5 cm primary nozzle was located at the middle of a 15 cm \times 5 cm secondary nozzle. The ratio between the secondary and primary velocities was fixed at $\lambda = 0.5$ most of the time, a value which is close to $\lambda = 0.4$ within the approximations made so far. Primary velocity was adjustable from 40 to 100 m/s. The secondary velocity ranged therefore between 20 and 50 m/s.

Experiments were made in the anechoic room of the Ecole Centrale de Lyon which is 6.10 m \times 4.60 m \times 3.80 m and has a cut-off frequency of 100 Hz [7]. The aerodynamic ducting already associated with the room was used to supply the secondary jet. It consists of three pairs of contra-rotating axial fans (mass flow rate 1.25 kg/s, maximum pressure 550 Pa), a 40 dB commercially available silencer (4 m long, 1 m² in section, with rockwool baffles), a 10 m duct with the same cross-section, followed by a second 40 dB silencer, a 7 to 1 contraction and a 2 m duct through the double walls of the room, and finally the 10 to 1 contraction upstream of the secondary nozzle.

The primary jet is supplied by an additional circuit consisting of a centrifugal fan (maximum mass flow rate 0.15 kg/s and pressure 18 000 Pa), a specially designed 40 dB silencer (cylinder 0.8 m diameter; length 1 m, with glasswool lining) a 30 m long flexible pipe 10 cm in diameter and a 2 to 1 contraction upstream of the nozzle.

The airfoil placed in the median jet was of the NACA 6512 A₁₀10 series, with a 8 cm chord and a 5 cm span. End plates were mounted flush with the nozzle edges. The angle of incidence was fixed at 0° (Figure 3).

All the far field acoustic measurements were obtained with a one-inch Brüel & Kjaer microphone located on the normal to the airfoil at 1.95 m from the airfoil. Preamplifier,

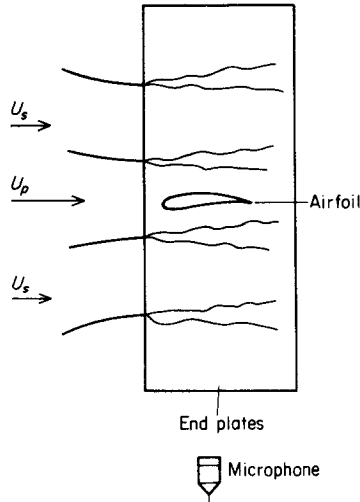


Figure 3. Experimental set-up.

amplifier and wave analyzer are standard Brüel & Kjaer equipment, types 2619, 2607 and 2020 respectively.

For the mean velocity and longitudinal component of the velocity fluctuations, a constant temperature anemometer was used (DISA type 55 D 01) with a hot wire probe DISA type 55 F 11.

4. RESULTS

4.1. NOISE OF THE ADJACENT JETS

In Figure 4 are compared the noise level of the adjacent plane jets and the noise level of the median jet alone for different velocities. For clarity of Figures 4, 6 and 9 to 14, the aerodynamic conditions are indicated on every curve by means of the letters J_1 , J_2 and A, which stand for primary jet, secondary jet and airfoil respectively. For example, $J_1 + A$ means that the airfoil is placed in the primary jet alone, and $J_1 + J_2 + A$ that the airfoil is placed in the adjacent jets system.

It can be observed from Figure 4 that the noise reduction obtained with the adjacent jets increases with velocity, being about 4.5 dB at 60 m/s and 7 dB at 100 m/s. This is associated with the lower rate of increase with velocity of the noise level of adjacent jets compared to single jets. In terms of power laws, the dependence is $U^{5.2}$ for adjacent jets and $U^{6.2}$ for single jets, for the velocity range investigated in our facilities. Such a behaviour can be expected because of (i) the low velocity range used for the primary jet; (ii) the even lower velocity range encountered for the secondary velocity and the velocity difference between the primary and secondary flows and (iii) the well established fact that for Mach numbers less than about 0.3 the exponent of the power law expressing the noise level dependence of single jets on velocity departs from 8 when the velocity is decreased [8, 9]. This acoustic behaviour of the adjacent jets is expected to persist until the Mach number of the secondary jet reaches 0.3. The 7 dB noise reduction observed at a primary velocity of 100 m/s would therefore be maintained for moderately higher values of this velocity, of the order of 150–200 m/s.

The acoustic efficiency e' measured for the adjacent plane jets set-up is plotted in Figure 5 for a primary velocity of 100 m/s and for different values of the velocities ratio λ around

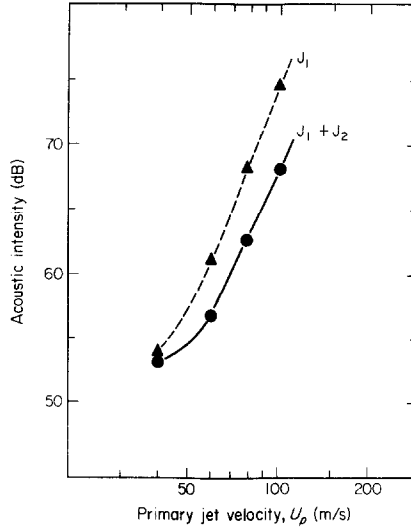


Figure 4. Comparison of the noise intensities of single and adjacent plane jets. ---▲---, Primary jet alone; —●—, adjacent plane jets ($\beta' = 2$; $\lambda = 0.5$).

$\lambda = 0.5$. These results agree within a reasonable extent with the theoretical curves deduced from expressions (5) and (6). Use is made of the experimental values of γ and δ obtained in the adjacent plane jets set-up (i.e., $\delta = 1$ and $\gamma = 1.7$ for $\lambda = 0.5$ and $\beta' = 2$). Two values of the power law exponent m which express the noise dependence on velocity of single jets have been used: $m = 7$ as in reference [6], and $m = 6$ which fits more closely the value $m = 6.2$ obtained with the present experimental set-up.

Finally, concerning the noise spectra of adjacent jets (see Figure 6), the essential feature is the large decrease of the contribution from all the preferred frequency range of emission of the median jet alone: for example, from 300 Hz to 2 kHz for $U_p = 100$ m/s and from 200 Hz to 1 kHz for $U_p = 40$ m/s, which corresponds to dimensionless frequencies in the range 0.2 – 1.1.

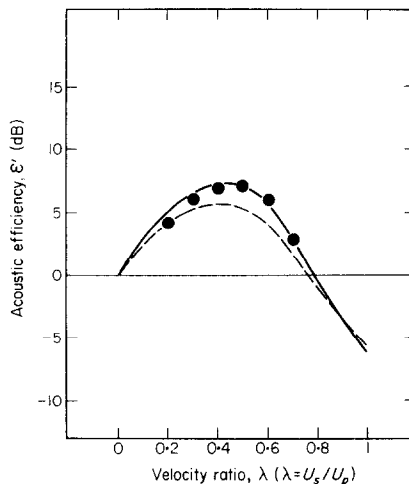


Figure 5. Estimated acoustic efficiency $\varepsilon'(\beta', \lambda)$ for the adjacent plane jets and comparison with experiments. —, Expressions (5) and (6) with $m = 7$; ---, expressions (5) and (6) with $m = 6$; ●, experiments.

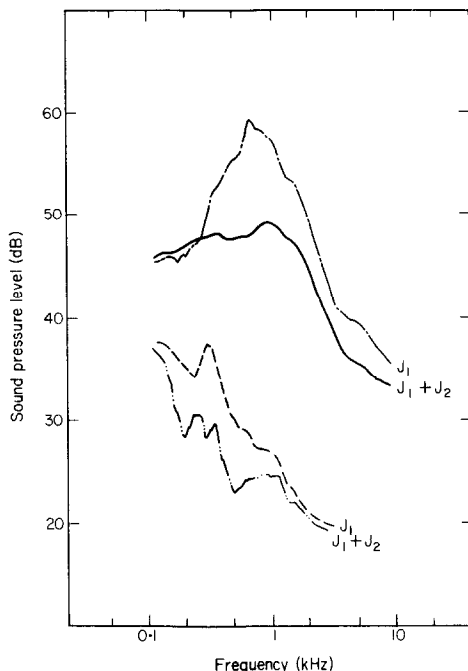


Figure 6. Comparison of the noise spectra of single and adjacent plane jets (bandwidth 31.6 Hz). —, Primary jet alone, $U_p = 100$ m/s; — — —, adjacent plane jets ($\beta' = 2, \lambda = 0.5$), $U_p = 100$ m/s; — · —, primary jet alone, $U_p = 40$ m/s; · · · ·, adjacent plane jets ($\beta' = 2, \lambda = 0.5$), $U_p = 40$ m/s.

4.2. LENGTH OF THE PRIMARY POTENTIAL ZONE OF THE ADJACENT JETS

The increase procured by the adjacent jets to the length of the primary potential zone appears clearly from Figure 7 in which are given the centre-line variation of the mean velocity along with that of the r.m.s. value of the longitudinal velocity fluctuations. The width of the potential zone was also determined from the flat central part exhibited by the

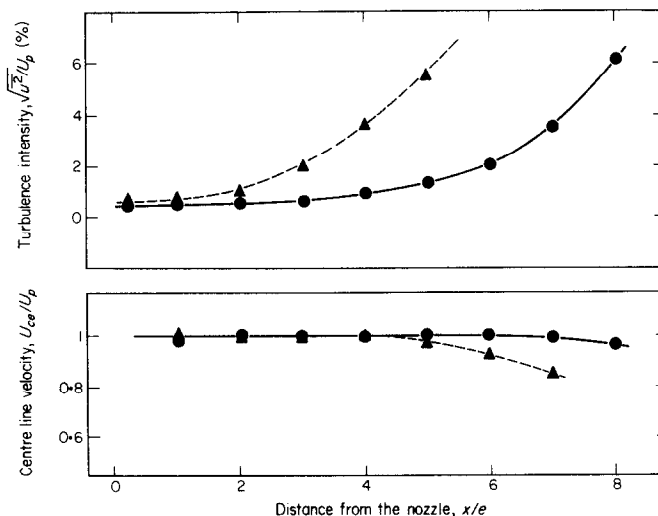


Figure 7. Downstream evolution of the centre line velocity and of the turbulence intensity (longitudinal velocity fluctuation). $U_p = 100$ m/s, primary nozzle width $e = 5$ cm, —●—, Adjacent plane jets ($\beta' = 2, \lambda = 0.5$); —▲—, primary alone.

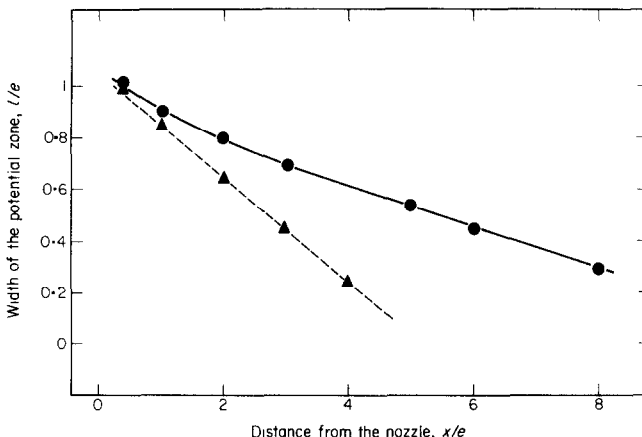


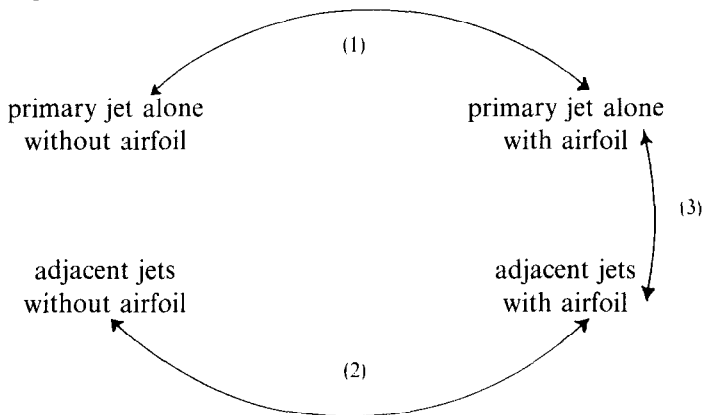
Figure 8. Downstream evolution of the width of the potential zone. $U_p = 100$ m/s. —●—, Adjacent plane jets ($\beta' = 2, \lambda = 0.5$); ---▲---, primary jet alone.

transverse profiles of the same quantities. Despite the usual inherent difficulty of edge location, the results (Figure 8) are in satisfactory agreement with those given in Figure 7.

A potential zone which is about twice as long as that corresponding to the primary jet alone is therefore produced in this set-up and will certainly hold for adjacent jets with larger aspect ratios (i.e., span to width).

4.3. NOISE EMITTED BY THE AIRFOIL

In order to appreciate the benefit of the adjacent jets set-up for the investigation of the airfoil aerodynamic noise, the acoustic level and the acoustic spectra were measured for the four following situations:



Comparisons were made as indicated by the arrows. For arrows (1) and (2) the sound emitted by the airfoil should be significantly higher than that of the jet set-up used. Along arrow (3) it would be expected that identical data be found. Now, from Figures 9 to 14 the following observations and deductions can be made.

- (i) The sound emitted by the airfoil exceeds the noise of the adjacent jets by a larger amount than it does the noise of the single primary jet (for example, at 100 m/s, 6.5 dB instead of 4.5 dB; see Figures 9 and 10). Of course, this can be expected from the result of section 4.1. but attention has also to be paid to another factor, as will be seen in what follows.

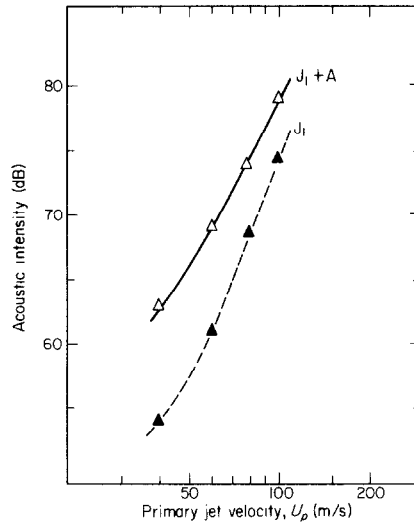


Figure 9. Noise intensity emitted by the airfoil when placed in a single jet. — \triangle —, Primary jet with airfoil; - \blacktriangle —, primary jet alone.

- (ii) The sound emitted by the airfoil seems more intense when the airfoil is located in the single primary jet than that emitted when it is in the primary jet of the adjacent jets. Although the shift is slight in the lowest part of the velocity range investigated, a drastic difference appears when the velocity reaches 60 m/s (Figure 11). An amplification seems therefore to affect the noise emitted by the airfoil and this is confirmed by the spectral measurements.
- (iii) The spectra given in Figure 12 reveal, indeed, that when the airfoil is introduced into the single primary jet, there is a marked increase of the noise at the preferred frequency of emission which already exists for the jet alone (see the circled areas in Figure 12 at $N \simeq 300$ Hz for $U_p = 40$ m/s, or $ND/U_p \simeq 0.40$, and at $N \simeq 700$ Hz for $U_p \simeq 100$ m/s, or $ND/U_p \simeq 0.35$).
- (iv) On the other hand, when the adjacent jets are used, it is possible to detect the specific spectra of the airfoil sound. In other words, the Strouhal emission

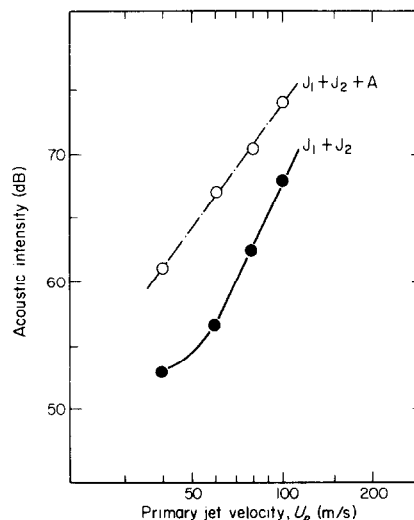


Figure 10. Noise intensity emitted by the airfoil when placed in the adjacent plane jets system. — \circ —, Adjacent plane jets with airfoil; — \bullet —, adjacent plane jets without airfoil.

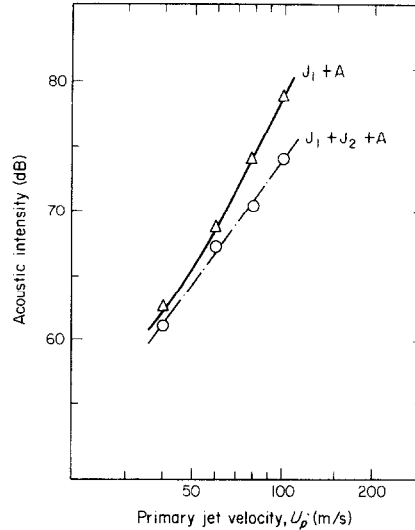


Figure 11. Comparison of the noise intensities emitted by the airfoil when placed in a single jet and in the adjacent plane jets system. — \triangle —, Primary jet with airfoil; — \circ —, adjacent plane jets with airfoil.

becomes apparent for $U_p = 40$ m/s as observed in previous measurements [10, 11] (see the circled areas in Figures 13 and 14, at $f \simeq 4$ kHz). The separated boundary layer on the positive pressure side of the airfoil could be responsible for the larger part of the noise spectra around $f \simeq 1.5$ kHz for $U_p = 40$ m/s and around $f \simeq 1.9$ kHz for $U_p = 100$ m/s. The adjacent jets set-up therefore removes, in a satisfactory way, the coupling which takes place between the incident flow and the airfoil when the section of the incident flow is not wide enough.

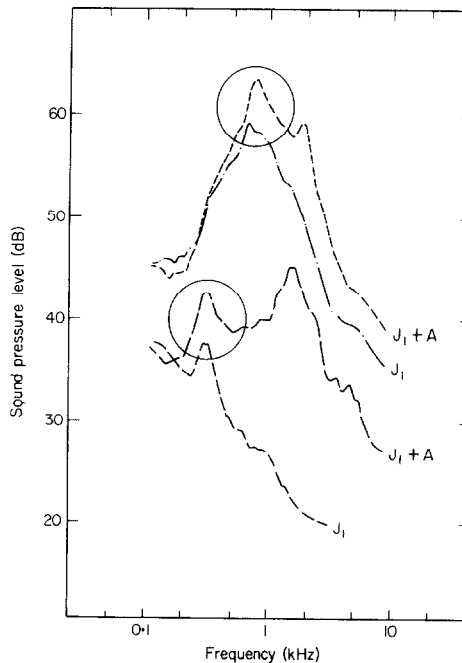


Figure 12. Noise spectra emitted by the airfoil when placed in a single jet, for two incident velocities (bandwidth 31.6 Hz). —, Primary jet with airfoil, $U_p = 100$ m/s; ---, primary jet alone, $U_p = 100$ m/s; —, primary jet with airfoil, $U_p = 40$ m/s; ---, primary jet alone, $U_p = 40$ m/s.

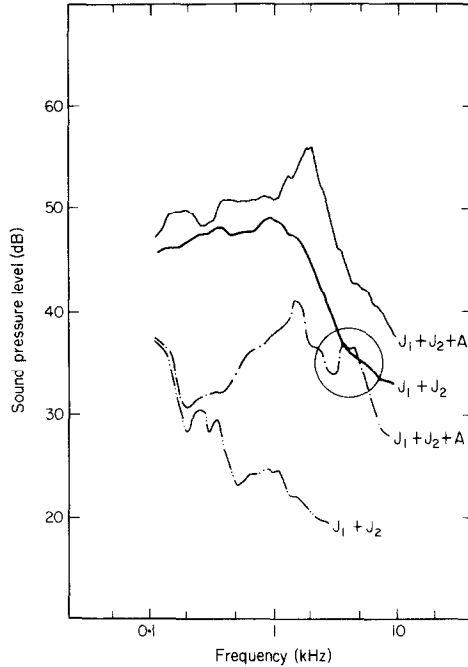


Figure 13. Noise spectra emitted by the airfoil when placed in the adjacent plane jets system, for two incident velocities (bandwidth 31.6 Hz). —, Adjacent plane jets with airfoil, $U_p = 100$ m/s; ---, adjacent plane jets without airfoil, $U_p = 100$ m/s; - · -, adjacent plane jets with airfoil, $U_p = 40$ m/s; · · ·, adjacent plane jets without airfoil, $U_p = 40$ m/s.

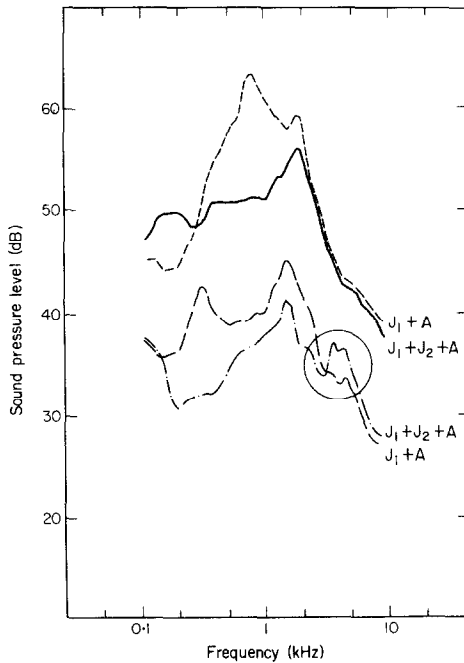


Figure 14. Comparison of the noise spectra emitted by the airfoil when placed in a single jet and in the adjacent plane jets, for two incident velocities (bandwidth 31.6 Hz). ---, Primary jet with airfoil, $U_p = 100$ m/s; —, adjacent plane jets with airfoil, $U_p = 100$ m/s; - · -, primary jet with airfoil, $U_p = 40$ m/s; · · ·, adjacent plane jets with airfoil, $U_p = 40$ m/s.

4.4. REFRACTION AND SCATTERING DUE TO THE MIXING LAYERS

The sound emitted by the airfoil has to pass through the shear layers of the adjacent jets to reach the far field microphone so that we have paid attention to two effects: (i) the refraction due to the mean velocity gradient which affects the measured angle of emission, the amplitude and the phase of the acoustic wave [12–14]; (ii) the scattering due to the turbulence which creates an attenuation, random phase fluctuations and a spectral broadening of the transmitted acoustic wave [14–16].

In order to have an upper bound of these effects we have made numerical estimates which apply to a possible extension of the present facility. We have therefore considered higher incident velocities ($U_p = 150$ m/s, $U_s = 75$ m/s) and longer chords of the airfoil ($c = 16$ cm). The width of the jet nozzles would then be 8 cm (Figure 15).

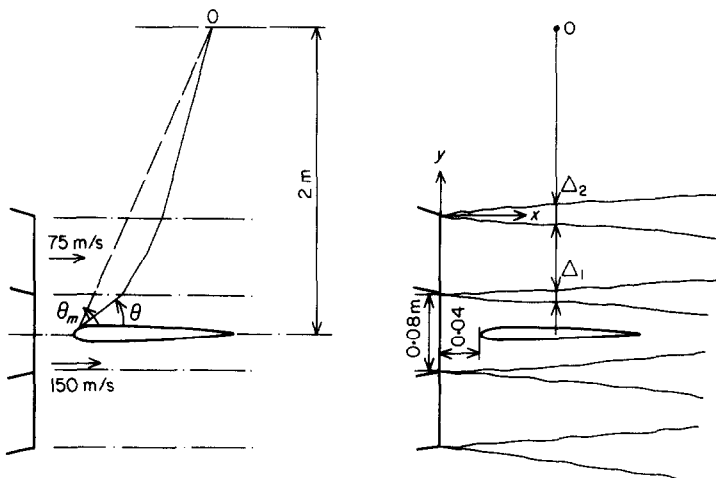


Figure 15. Main parameters used for estimating the corrections associated with the refraction and scattering effects.

The refraction effects have been estimated from the velocity difference between the central jet and the fluid at rest since that velocity jump is the relevant parameter of the problem [12]. The results are as follows.

- (i) The correct emission angle θ' can be deduced from the observation angle θ_m by adding a deviation which is nearly constant and equal to $30^\circ \pm 1^\circ$, when θ_m lies in the range $70^\circ \lesssim \theta_m \lesssim 110^\circ$.
- (ii) In the same range of θ_m and for an observer located at 2 m above the airfoil, a difference of only 0.8 dB appears between two acoustic signals which originate from the trailing edge and the leading edge respectively (from equation (5) in reference [12]).
- (iii) The level and phase changes detected by the extreme microphones of an acoustic antenna are large. As an example, if a linear antenna of 1 m is used at 2 m from the airfoil, the difference would be about 6 dB. However, all these changes are deterministic so that they can be checked by means of a known source and introduced in the data processing.

To estimate the scattering, the main parameters of the turbulence (turbulence level u' : length scale L) have been approximated by

$$u'/(U_p - U_s) \simeq 0.18, \quad A \simeq 0.06x, \quad L \simeq A/2$$

in the internal mixing layer, and by

$$u'/U_S \simeq 0.18, \quad \Delta \simeq 0.12x, \quad L \simeq \Delta/2$$

in the external mixing layer. Furthermore, the effects of the two shear layers are assumed to be uncorrelated. The acoustic frequency we considered is $f = 3$ kHz, a value which seems an upper limit for the airfoil noise (extrapolation of the spectra given in Figure 13 and of the dominant range of emission when inhomogeneities are added to the incident flow [17]). Accordingly the estimates for the scattering effects are as follows.

- (i) The attenuation of the coherent wave proposed in reference [15] and quite well verified by experiments gives

$$\langle p \rangle = p_0 \exp\{-k_0^2(u'^2/c_0^2) L\Delta\} \simeq 0.06 \text{ dB.}$$

- (ii) The phase fluctuation evaluated in reference [16], which is also in good agreement with experiments, is

$$\sqrt{\phi'^2} = (u'/c_0) k_0 \sqrt{L\Delta} \simeq 5.2^\circ.$$

- (iii) The spectral broadening would only appear at a very low level, around -35 dB.

It is therefore possible to neglect all transmission effects, except for the refraction associated with the mean field. The latter phenomenon, however, can in principle, at least, be easily taken into account since it is purely deterministic.

5. CONCLUSION

The aerodynamic sound emitted by airfoils is much more efficiently detected when adjacent plane jets are used, in preference to single jets, to generate the incident flow ducted into the anechoic room. In addition to the expected benefit in the acoustical conditions of the experiments (decrease of the background noise level of the adjacent jets, especially at high speeds, and shift of their spectra towards frequencies below the range of interest for the airfoil emission), there are improvements in the aerodynamic conditions (increase in size of the potential zone, suppression of induced flow fluctuations, and hence the possibility to study airfoils with longer chords).

Feasibility experiments were made on a small scale set-up which gave Reynolds numbers based on the airfoil chord up to 5×10^5 . In a larger set-up, a factor of two is expected to be gained both on the airfoil chord and on the incident flow velocity, so that Reynolds numbers of the order of 2×10^6 would be achieved. In this larger set-up the aspect ratio of the jets could be also increased (by a factor of three) in order to improve the two-dimensionality of the flow considered. In addition, values of the secondary to primary velocities ($\lambda = 0.5$) and of the secondary to primary areas ($\beta' = 2$) are such that the cost of building a full experimental facility would be kept within reasonable limits.

ACKNOWLEDGMENTS

This work has been supported by the Service Technique de l'Aéronautique under research contract No. 7793311.

REFERENCES

1. T. F. SIDDON 1973 *Journal of the Acoustical Society of America* **53**, 619–633. Surface dipole strength by cross correlation method.
2. P. J. F. CLARK and H. S. RIBNER 1969 *Journal of the Acoustical Society of America* **46**, 802–805. Direct correlation of fluctuating lift and radiated sound for an airfoil in turbulent flow.
3. R. K. AMIET 1975 *Journal of Sound and Vibration* **41**, 407–420. Acoustic radiation from an airfoil in a turbulent stream.
4. B. D. MUGRIDGE 1971 *Journal of Sound and Vibration* **16**, 593–614. Acoustic radiation from aerofoils with turbulent boundary layers.
5. S. S. DAVIS 1975 *American Institute of Aeronautics and Astronautics Paper No. 75-488*. Measurements of discrete vortex-noise in a closed throat wind tunnel.
6. D. JUVE, J. BATAILLE and G. COMTE-BELLOT 1978 *Journal de Mécanique Appliquée* **2**, 385–398. Bruit de jets coaxiaux subsoniques.
7. J. P. BERHAULT, M. SUNYACH, H. ARBEY and G. COMTE-BELLOT 1973 *Acustica* **29**, 69–78. Réalisation d'une chambre anéchoïque revêtue de panneaux et destinée à l'étude des bruits d'origine aérodynamique.
8. P. A. LUSH 1971 *Journal of Fluid Mechanics* **46**, 477–500. Measurements of subsonic jet noise and comparison with theory.
9. D. JUVE, M. SUNYACH and J. BATAILLE 1976 *Comptes Rendus de l'Académie des Sciences de Paris* **283B**, 269–272. Application de la méthode de causalité à l'étude du bruit d'un jet subsonique.
10. R. W. PATERSON, P. G. VOGT, M. R. FINK and C. L. MUNCH 1972 *American Institute of Aeronautics and Astronautics Paper No. 72-656*. Vortex noise of isolated airfoils.
11. M. SUNYACH, H. ARBEY, D. ROBERT, J. BATAILLE and G. COMTE-BELLOT 1973 *AGARD Conference No. 131, Noise Mechanisms, Paper No. 5*. Correlations between far field acoustic pressure and flow characteristics for a single airfoil.
12. R. K. AMIET 1975 *A.I.A.A. 2nd Aeroacoustic Conference, Paper No. 75-532*. Correction of open jet wind tunnel measurements for shear layer refraction.
13. R. K. AMIET 1978 *Journal of Sound and Vibration* **58**, 467–482. Refraction of sound by a shear layer.
14. S. CANDEL, A. GUEDEL and A. JULIENNE 1975 *Sixième Congrès International sur l'instrumentation dans les installations de simulation aérospatiale, Ottawa*. Refraction and scattering of sound in an open wind tunnel flow. (See also *ONERA TP* 1975–79.)
15. A. R. WENZEL and J. B. KELLER 1971 *Journal of the Acoustical Society of America* **50**, 911–920. Propagation of acoustic waves in a turbulent medium.
16. L. A. CHERNOV 1960 *Wave Propagation in a Random Medium*. New York: McGraw-Hill.
17. H. ARBEY, M. SUNYACH and G. COMTE-BELLOT 1977 *Proceedings 6th Canadian Congress of Applied Mechanics* 781–782. Effet d'une pré-turbulence sur le bruit aérodynamique des profils d'aube.